Energy & Buildings 254 (2022) 111562

Contents lists available at ScienceDirect

Energy & Buildings

journal homepage: www.elsevier.com/locate/enb

Thermal comfort prediction of the existing housing stock in southern Spain through calibrated and validated parameterized simulation models

Carmen María Calama-González *, Rafael Suárez, Ángel Luis León-Rodríguez

Instituto Universitario de Arquitectura y Ciencias de la Construcción, Escuela Técnica Superior de Arquitectura, Universidad de Sevilla, Av. Reina Mercedes 2, Seville 41012, Spain

ARTICLE INFO

Article history:
Received 28 May 2021
Revised 5 October 2021
Accepted 8 October 2021
Available online 13 October 2021

Keywords:
Social housing stock
Building stock modelling
Thermal comfort
Bayesian calibration
Bottom-up
Mediterranean climate

ABSTRACT

Due to 2030 and 2050 targets of the latest international standards, energetically retrofitting the existing building sector requires special attention. Prior to the proposal of retrofit strategies, it is necessary to analyse the current energy performance of the stock. Although simulation tools provide accurate results of energy performance at the building level, individual assessments of the large-scale stock lead to extensive data collection and huge computational resources. This paper assesses the current performance of one of the most representative building typologies in social housing stock in southern Spain, the H-typology, predicting results on indoor thermal comfort at the stock level. The physical, constructive and geometrical building characterisation and the selection of a calibrated and validated case study through monitoring are used to generate parameterized energy simulation models, providing statistically representative samples of the stock. Open-access energy simulation tools have been combined with statistical software. Conclusions reported show average annual discomfort hours of around 68%, with higher percentage of annual undercooling discomfort hours, and identify the most influential parameters on indoor thermal comfort as infiltration rate, people density and night-time natural ventilation rate. Moreover, 10 Latin Hypercube Samples per parameterized variable derived in highly representative results for thermally analysing the stock.

1. Introduction

In 2020, as a result of global warming, the average surface temperature increased by 1.02 °C compared to 1951–1980 [1]. Given the urgent need to tackle the potential future effects of climate change, several European regulations have recently been updated to demand new energy consumption and efficiency targets [2], with the building sector considered a major priority. European building stock accounted for approximately 36% of carbon emissions and 40% of the total energy consumption [3]. Given that the current annual new-built construction rate is below 2% [4], retrofit solutions for improving energy efficiency in existing buildings must be promoted as a vital objective to meet the proposed energy goals. In Europe, building renovation could reduce total energy consumption and CO_2 emissions by 6% and 5%, respectively [5].

The assessment of the current state of the existing building stock and its thermal and energy performance is a key aspect prior to any energy saving measure [6]. As much of the housing stock was built under no energy performance obligation and is expected to make up a large part of the future building stock, large-scale procedures to enhance energy building efficiency must be prioritized in the coming years [7]. In this regard, building energy modelling (BEM) through dynamic simulation is a useful tool for the accurate estimation of the thermal performance of buildings [8], along with the assessment of the effects of retrofit and technology incentives. These provide interesting implications for decision-making in the design and operation stages [9]. However, proposing energy efficiency measurements which are not based on calibrated and validated simulation models may lead to uncertain predictions and results which are not adjusted to the real building performance [10], noticeably increasing the performance gap [11].

Despite limitations such as model complexity, lack of extensive data, high computation time and methodological uncertainties [12], Building Stock Modelling (BSM) has commonly been used to assess large-scale building energy performance. According to Swan and Ugursal [13] building stock modelling approaches can be classified into two groups: top-down or bottom-up. Top-down methods assess cities at a macro scale, examining the technological and economic effects. However, the use of historical aggregated

* Corresponding author.
E-mail address: ccalama@us.es (C.M. Calama-González).

https://doi.org/10.1016/j.enbuild.2021.111562
0378-7788/

data results in a significantly limited technique for accurate modelling on an hourly basis, generally simulating macro-data on a yearly or monthly resolution [14]. In contrast, bottom-up models consider urban and building attributes at the micro-scale, relying on extensive data and extrapolating the performance estimation to a regional or national context [15]. While these approaches display greater accuracy, they require high computational burdens [14]. There are two bottom-up methodology categories: data-driven approaches, which use historical building stock information to correlate relationships between input–output data through statistical techniques [16], and engineering or simulation methods, which use archetypes that represent various building types of the stock [17]. An archetype or "statistical composite of the features found within a category of buildings in the stock" [18] can be characterised by a set of properties statistically detected in a building category [19]. Thus, a stock model can be created from a large empirical database using a bottom-up method by defining archetypes [20].

Using top-down methodologies for stock performance assessment, Farzana et al. [21] estimated future energy consumption for urban areas of Chongqing, using the Matlab environment to compare artificial neural networks with other regression and polynomial models. Relevant socio-economic and primary data of Chinese buildings are collected using questionnaires and incorporated into the model. Likewise, Mikkola et al. [22] obtained spatial and input data from statistics databases to apply a top-down method and generate spatio-temporal energy load profiles for two cities (Helsinki and Shanghai).

In contrast, Krarti et al. [23] predicted energy consumption of the residential building stock in Saudi Arabia to propose retrofit programs through a bottom-up simulation approach, using DOE-2.2 freeware building energy software. 54 prototypes were constructed with building characteristics obtained from surveys and databases (construction materials, lighting loads, HVAC systems, window glazing properties...). Mastrucci et al. [16] estimated energy consumption of the residential stock in Rotterdam through a bottom-up statistical and validated model implementing multiple linear regression. These authors coupled Geographic Information System (GIS) software with the R statistical tool, incorporating dwelling information (type, floor surface, number of occupants, envelope properties...) in order to assess the energy saving potential of several retrofit solutions. Österbring et al. [24] used a bottom-up GIS model linked with Simulink/Matlab software to obtain energy consumption for the city of Gothenburg, incorporating urban information from public databases and historical building regulations (such as HVAC systems, number of stories, construction year, U-values...). Mata et al. [6] used a bottom-up engineering model applied to a national scale. Also through Simulink/Matlab environments, these authors estimated the final energy performance of buildings in four countries, defining archetype buildings based on physical and thermal aspects (inertia, HVAC systems, climate conditions...) obtained from scientific literature. Ascione et al. [25] analysed around 500 buildings in the city of Benevento using a GIS tool to obtain energy consumption results. To do so, geometry, thermo-physical properties of envelopes and average HVAC data for buildings were obtained from audits, other studies and normative or cartographic documents. Issermann et al. [26] analysed energy demand and potential energy saving of the residential building stock of Wuppertal (Germany) in a future scenario, incorporating building properties from the TABULA project [27]. Nägeli et al. [28] and Oberegger et al. [29] have also recently proposed bottom-up stock modelling to predict energy demand and energy-saving for several retrofits, presenting a useful tool for cost-effective policy evaluation applied to residential building stock.

A smaller number of authors propose hybrid methods, using data from local building archetypes as input in dynamic building energy models. Brøgger et al. [30] applied a multiple linear regression hybrid model, validated through statistical measures, to determine the energy-saving potential of the Danish residential building stock. The model incorporated information on building elements, orientation, size, ventilation/infiltration rates, etc. obtained from Energy Performance Certificates and Building Register databases. Swan et al. [13] followed an engineering approach combined with a neural network method to predict energy consumption of the Canadian housing stock, incorporating the outputs of the statistical model into the stock building-physics based simulation model. Fonseca et al. [31] generated a hybrid method coupling Python energy simulation software and ArcGIS tool to assess the energy demand, carbon and financial benefits of different retrofit strategies applied to a neighbourhood in Switzerland through multi-criteria decision analysis. To do so, these authors included urban and building properties (including window-to-wall ratio, height, shading systems, envelope and HVAC systems) contained in public databases.

Nonetheless, according to Brøgger et al. [30], indoor environmental conditions must be known in order to propose realisable energy-saving potential measures in the existing stock, in addition to the building physical properties. This is particularly important in southern Spain, given the generalized lack of Heating, Ventilation and Air Conditioning (HVAC) systems in the social housing stock, due to occupants' low socio-economic resources [32]. Therefore, the major challenge is not the reduction of energy demand in the social dwellings of southern Spain, but rather the improvement of indoor comfort conditions, as energy waste is lower than expected in many of these buildings [33].

As stated above, most of the publications analysing the existing residential building stock focus on energy demand and consumption assessment, so more extensive research on the performance of the existing building stock towards indoor comfort conditions is still required. Dino et al. [34] coupled EnergyPlus and Matlab to obtain results on the energy use, CO_2 emissions and occupant comfort (according to ASHRAE 55:2004 [35] and EN 15251:2007 [36]) of the residential building stock in four Turkish cities. Their ultimate objective was the assessment of energy-saving retrofit solutions towards 2060 climate change. However, to do so, these authors calculate building envelope and element properties based on Turkish standards, which they later included as input into the building stock models, instead of using statistical information from building stock databases. Palma et al. [37] used a GIS environment to build a bottom-up methodology to compute the theoretical final energy consumption of the Portuguese building stock, combined with a top-down approach to estimate real final energy consumption, based on meeting comfort conditions, even though no comfort analysis was reported. These authors admitted that the model did not "perfectly encompass the true diversity" of the building stock, since the building characteristics considered (envelope, glazing and window type, geometrical and physical properties) have been set at fixed average values.

The ultimate aim of this paper is to address the literature gap identified on the assessment of the current performance of the existing social housing stock towards indoor comfort conditions. Moreover, comfort results predicted by the simulation tool are assessed according to the recently published adaptive comfort model included in EN 16798–1:2019 [38] (which replaces EN 15251:2007 [36], analysed in similar studies conducted so far). A hybrid bottom-up methodology is proposed to assess the current performance of social housing stock in southern Spain (Mediterranean climate), combining data-driven techniques and simulation methods, which allow the development of energy models or archetypes statistically representative of the existing building stock. Although previous analysis on the performance of the building stock of the Mediterranean area has been carried out, it has been focused on the linear building typology [32], which only represents

35% of the social housing dwellings in southern Spain, where there is a higher percentage of H-typology housing buildings (45%).

Compared to other studies mentioned above, this paper selects a case study among the analysed H-typology building stock and constructs an energy simulation model, which is calibrated and validated through on-site monitoring hourly data. In order to construct stock energy models, the case study energy model is later parameterized, incorporating the statistical analysis results of a large building database, which include physical, constructive, typological and geometrical information of the building housing stock. Open access energy simulation and statistical tools are used throughout the whole process.

This paper is divided into several sections: the methodology, described in Section 2, includes the theoretical and normative fundaments, and a description of the tasks followed; the analysis and results discussion is presented in Section 3; while the strengths and limitations of this work are included in Section 4, along with future research possibilities. Finally, the conclusions of this paper are reported in Section 5.

2. Methods

This paper presents an analysis on the current state of social housing building stock in southern Spain (Mediterranean climate), assessing its current performance on indoor thermal comfort. To do so, on-site monitoring techniques are combined with building modelling through energy simulation tools and statistical methods for data processing, treatment and analysis.

The methodology followed has been divided into several stages (Fig. 1), described in the following subsections: 1. Building stock characterisation. Representative samples; 2. Case study selection. On-site monitoring; 3. BEM Parameterization; 4. BEM Sensitivity analysis; 5. BEM Calibration and validation; 6. BSM Parameterization; 7. BSM Thermal comfort assessment; and 8. BSM Sensitivity analysis.

2.1. Building stock characterisation. Representative samples

The first step in the performance assessment of buildings at stock level is the detailed building characterisation, from a typological, morphological, constructive and energy points of view. In this case, information contained in a public database, originally developed by the Andalusian Agency for Housing and Retrofitting (AVRA) [39], has been used. This database includes several aspects from 39,486 social public dwellings in southern Spain, among which 77.5% are classified as multi-family housing buildings. The content of this database has been improved and expanded with additional information obtained from the Spanish cadastre online platform [40] and the Spanish Building Technical Code [41]. The current database includes general information (cadastral reference, address); building data (orientation, climatic zone, building height, average floor area, total built area, number of storeys, number of dwellings, year of construction, building urban and architectural typology - i.e. linear block, H, tower… grouped as collective closed blocks, terraced, isolated…); retrofit information (year and type of intervention); and energy-related data, such as building systems; constructive description of the envelope or annual energy cooling and heating demand. This database has been analysed statistically [42] in order to characterise the existing building stock. After identifying the predominant building typologies of the social housing stock in southern Spain based on the analytical results obtained one of the predominant building typologies, the H-typology, was selected, which represents around 13,890 social dwellings, in contrast to approximately 10,715 linear-typology buildings. The most representative parametric ranges of this stock have been statistically defined (included in section 2.6) using the statistical tools of Microsoft Excel® [43], R v.3.5.3 [44] (free software for statistical computing and graphics) and the QGIS v.2.18 [45] planimetric tool (an open-access public platform which allows the visualisation and regionalisation of spatial data).

2.2. Case study selection. On-site monitoring

Based on the data included in the AVRA public housing database on social dwellings in southern Spain, a case study has been selected from the H-typology buildings based on the statistical analysis conducted. The case study selected corresponds to a 4-storey high block, built in 1973 with four dwellings per floor (Fig. 2).

The building is located in Córdoba, in southern Spain, a Mediterranean area located in the "B4" climatic zone according to the Spanish Building Technical Code [41]. This code defines the Climatic Severity in Winter (SCI) with a letter ("A" corresponds to milder winters, while "D" refers to colder winters) and the Climatic Severity in Summer (SCV) with a number ("1" represents areas with milder summers while "4" refers to warmer summers) (Table 1). In the B4 climatic zone, the H-typology represents 61.4% of the social dwellings, while the linear and tower typologies account for 34.3% and 4.3%, respectively.

In addition to compiling planimetric information and physical, constructive and morphological data on the case study (summarized in section 2.6), on-site monitoring was carried out on several ambient variables in the building for a prolonged period of time [46]. One of the dwellings on the third floor was monitored during a 10-month period (from 1 June to 31 March), recording hourly measurements for air temperature, both indoor (in the living room and main bedroom) and outdoor. Thus, on-site measurements were carried out during different seasonal periods (summer, winter and mid-season) in the occupied house (couple with two children). Due to limitations imposed by users, it was not allowed to collect specific thermal comfort data or surveys during the 10-month monitoring process. It should also be noted that this dwelling has no mechanical ventilation systems, only cross natural ventilation through windows.

2.3. BEM parameterization

In this stage, a BEM of the case study was constructed based on its physical, constructive and geometrical characteristics (section 2.6), using energy simulation tool and engine EnergyPlus v.9.0.1 [47], an open-source for building energy modelling. In addition, outdoor air temperatures recorded during the monitoring period were imported into the weather file (.epw) of the energy simulation tool.

The energy and ambient performance of simulation models of existing buildings often differs significantly from reality due to different factors (software limitations, input inaccuracy, users' building operation, etc.), leading to an inevitable performance gap [48]. Therefore, any energy simulation model analysing the performance of existing buildings must be subjected to a calibration and validation process, comparing simulated data with on-site measurements until acceptable differences are reached [49]. To ease this task, a parameterization was conducted on several variables included in the BEM, coupling EnergyPlus with jEPlus v.1.7.2 [50]. This step has allowed the automatisation of the subsequent tasks, optimizing computational time and the efficient use of available resources for data processing and analysis.

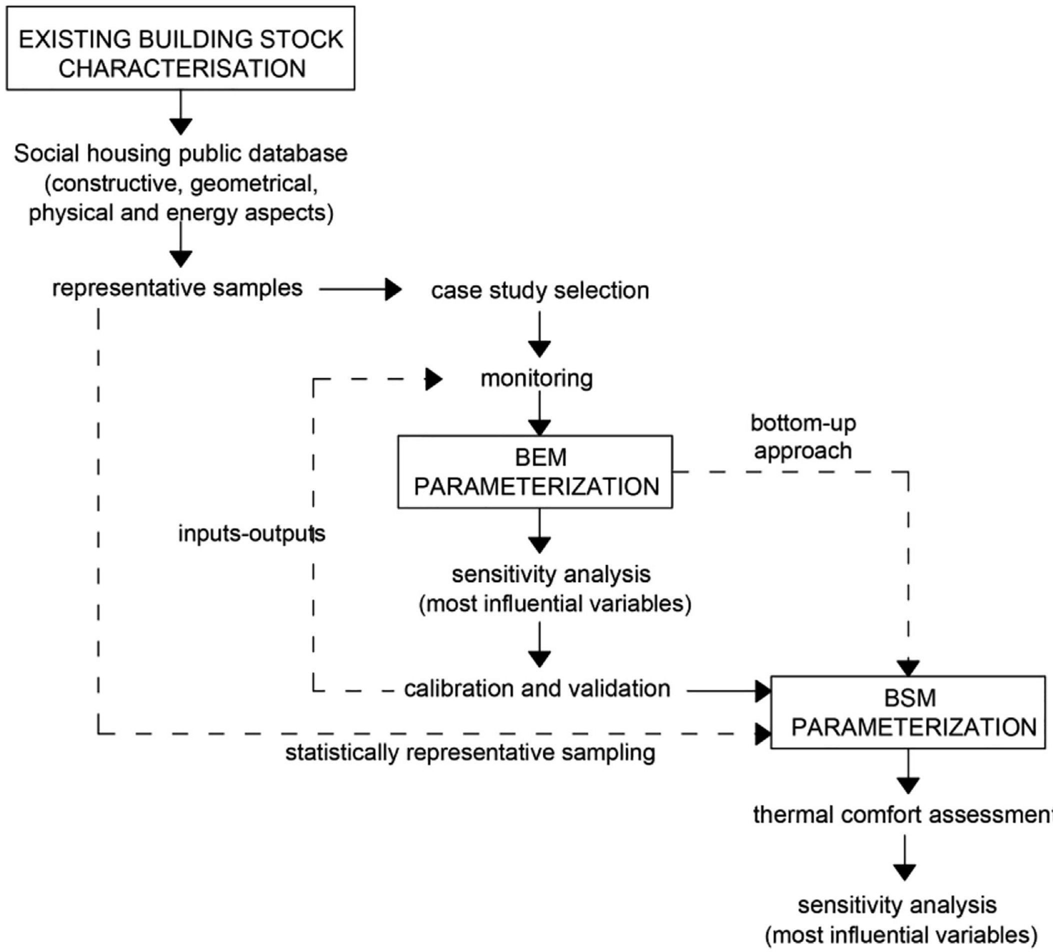

Fig. 1. Methodology followed: work stages.

2.4. BEM sensitivity analysis

Once the BEM of the case study is modelled and parameterized, this phase includes a first sensitivity analysis to identify the most influential parameters on simulation results due to modifications in the input settings. This task focuses calibration efforts of the case study BEM on the most important parameters, as calibrating every single parameter of the model would be considered a poor use of time and resources [51]. Thus, sensitivity analysis reduces the number of calibration parameters, and in turn, of computational burdens.

Given the ultimate objective of this research and the fact that users only allowed data on indoor and outdoor air temperatures to be collected, the most influential variables of the case study BEM on indoor air temperatures have been established. The top-four most influential variables are those subjected to the calibration process until the adjustment between simulated outputs and on-site air temperature measurements is validated following international standards (section 2.5). It should be highlighted that, even though no comfort data assessment was conducted during the monitoring period on the case study, calibrating the BEM with respect to indoor air temperatures provides an adequate approach for the subsequent thermal comfort prediction, given that adaptive comfort models are considered (section 2.7), which take into account both indoor and outdoor thermal criteria.

In this study, the parameter screening technique used is the Morris method [52], later extended by Campolongo et al. [53], and extensively applied in BEM [54,55]. This technique allows the value to be changed, one parameter at a time, maintaining the remaining variables as fixed values, in order to assess its influence on output results, making it a one-step-at-a-time approach. Finally, analysed variables are classified according to relative effect on the reported output, taking into account two parameters: the standard deviation (σ), which measures the parameter's interaction with the remaining variables; and the modified mean (μ^*), which quantifies the impact of the parameter on the simulation output. An extensive description of this screening method can be found in [56]. The Morris method has been implemented through the statistical software R v.3.5.3 [44].

2.5. BEM calibration and validation

This stage includes all the tasks for the calibration of the BEM of the case study. The energy simulation model variables calibrated are the top-four most influential parameters on indoor air temperatures, obtained from the sensitivity analysis developed in the previous phase. Selecting a higher number of calibration parameters would lead to higher computation time and a loss of posterior precision [57], ultimately resulting in a poor-quality simulation model.

Bayesian calibration techniques [58] have been implemented, as this approach allows the consideration of parameter uncertainties, based on the definition of prior distributions for input parameters. In other words, these distributions include the most likely range of the possible values of the calibration parameters. This technique provides advantages such as the easy incorporation of

(a) (b)

Fig. 2. Case study: (**a**) General views (©Google Street View); (**b**) Floor plans.

Table 1
Climatic zones established in the Spanish Building Technical Code [41]. Climatic zones of southern Spain are represented in bold.

Climatic severity	Parameter	Range	Climatic zones
SCI = a·R_i + b·G_i + c·R_i·G_i + d·R_i^2 + e·G_i^2 + f	A	SCI $\leq$ 0.3	**A3**, **A4**, **B3**, **B4**, C1, C2, **C3**, **C4**, D1, **D2**, **D3**, E1
	B	0.3 < SCI $\leq$ 0.6	
	C	0.6 < SCI $\leq$ 0.95	
	D	0.95 < SCI $\leq$ 1.3	
	E	SCI > 1.3	
SCV = a·R_v + b·G_v + c·R_v·G_v + d·R_v^2 + e·G_v^2 + f	1	SCV $\leq$ 0.6	
	2	0.6 < SCV $\leq$ 0.9	
	3	0.9 < SCV $\leq$ 1.25	
	4	SCV > 1.25	

R_i: cumulative average global solar radiation in January, February and December [kWh/m^2]
G_i: average of the degree-day in winter in base 20 for January, February and December. Determined on an hourly basis for each month and divided by 24.
R_v: cumulative average global solar radiation in June, July, August and September [kWh/m^2]
G_v: average of the degree-day in summer in base 20 for June, July, August and September. Determined on an hourly basis for each month and divided by 24.
a to f: specific coefficients for SCI and SCV, included in the Code's appendix.

prior information, capability to compute probabilistic results as reasonable expectations; and the possibility to include different sources of uncertainties (model inputs, discrepancies due to limitations of building modelling software, errors in field observations…). In view of this, in recent decades Bayesian techniques have become one of the most favourable calibration methods [59], increasingly applied to BEM [60,61].

This task has also been carried out using R v.3.5.3 [44] software. A more detailed description of the methodological process followed during the Bayesian calibration can be found in [56].

Once the BEM of the case study is calibrated, it is validated by comparing the simulated outputs with monitored data on indoor air temperatures. The most common uncertainty indices used to assess the accuracy of a calibrated model are defined in ASHRAE Guideline 14:2002 [62]: the Normalized Mean Bias Error (NMBE), the Coefficient of Variation of the Root Mean Square Error (CVRMSE) and the Coefficient of Determination (R^2) (Equations (1) to (3)).

$$\mathrm{NMBE} = \frac{1}{\bar{m}} \hat{A} \cdot \frac{\sum_{i=1}^{n}(m_i - s_i)}{n - \rho} \hat{A} \cdot 100(\%) \tag{1}$$

$$\mathrm{CV(RMSE)} = \frac{1}{\bar{m}} \hat{A} \cdot \sqrt{\frac{\sum_{i=1}^{n}(m_i - s_i)^2}{n - \rho}} \hat{A} \cdot 100(\%) \tag{2}$$

$$R^2 = \left(\frac{n\hat{A} \cdot \sum_{i=1}^{n} m_i \hat{A} \cdot s_{i-} \sum_{i=1}^{n} m_i \hat{A} \cdot \sum_{i=1}^{n} s_{i\hat{A}\cdot}}{\sqrt{\left(n\hat{A} \cdot \sum_{i=1}^{n} m_i^2 - \left(\sum_{i=1}^{n} m_i\right)^2\right)\hat{A} \cdot \left(n\hat{A} \cdot \sum_{i=1}^{n} s_i^2 - \left(\sum_{i=1}^{n} s_i\right)^2\right)}} \right)^2 \tag{3}$$

Where:
m_i: measured values
s_i: simulated data
n: number of measured data points
ρ: number of adjustable model parameters
$\overline{m}$: mean of measured values

According to the aforementioned Guideline, differences between simulated and monitored data are reasonably small if the three metrics are below the thresholds shown in Table 2.

2.6. BSM parameterization

This phase focuses on the parametric representation of the existing social housing stock of southern Spain in order to later estimate its thermal performance in current conditions. Once the case study BEM has been calibrated and validated, it has been used as the baseline to develop parameterized energy simulation stock models which are representative of the existing housing stock, BSM, applying a hybrid bottom-up approach. To do so, building archetypes have been created, with physical, constructive and geometrical properties defined based on the variation ranges obtained in the building characterisation of the selected stock (section 2.1).

Table 3 shows the variation ranges defined in the building characterisation of the stock for different physical, constructive, geometrical and operational variables, that is, the results of the statistical analysis conducted on the social public housing database of AVRA for the H-typology in Spanish Climatic Zone B4 (BSM) in its current state. This table also includes the specific values of these variables for the selected case study (BEM).

The parameterization of the energy simulation model was included into the EnergyPlus code (.idf and .imf files), through the EP-macro option. The geometry of the building was parameterized in three dimensions (X, Y and Z), so each construction element (wall, roof, window…) has several parameterized vertices which correspond to the spatial position of each corner of the specific element. When building floor area is modified from one model to the next one during simulations, the variables parameterized are changed proportionally, compared to the original's model geometry. Window-to wall ratio is also changed proportionally to the building's original geometry.

Latin Hypercube Sampling (LHS) has been implemented to build the simulated set corresponding to the BSM and to analyse its current thermal performance. Input distribution is divided into N intervals, combining individual modelling parameters with at random [63] to create samples in the multi-dimensional space with an equal probability [64]. According to Pang et al. [65], LHS provides more stable results than those obtained with simple random sampling and is easier to implement than the stratified sampling method. In terms of application in buildings, several studies implement LHS for calibration and simulation processes at both building [66,67] and stock [68,69] levels, for sampling modelling parameters (orientation, envelope properties, occupancy, ventilation and infiltration rates, HVAC characteristics, etc.).

Scientific reasoning [70] suggests that it would be enough to consider a minimum of 10 LHS samples per parameterized variable. Thus, the minimum number of simulations to efficiently assess the social housing stock selected would be 250, since there are 25 parameterized variables (P1 to P25). Nevertheless, to ensure the representativeness of the cases and following the recommendations mentioned by Escandón et al. [71] regarding the validation of the parameterized model, a comparative analysis has been carried out for the results obtained for different numbers of simulated cases: 250, 500, 750 and 1000 simulations (10, 20, 30 and 40 LHS, respectively). The aim of this to determine whether considering a sample of 10 LHS per parameterized variable would be enough to adequately assess the residential stock mentioned.

Table 2
Uncertainty ranges according to ASHRAE Guideline 14:2002 [62].

Calibration Frequency	Index	ASHRAE
Monthly	NMBE	±5%
	CV(RMSE)	15%
Hourly	NMBE	±10%
	CV(RMSE)	30%
Suggested	R^2	>0.75

2.7. BSM thermal comfort assessment

In order to carry out the indoor thermal comfort analysis, the statistical adaptive model included in the EN 16798–1:2019 [38] international standard has been considered. This model is applied to buildings under free-running conditions, with low metabolic rate, where occupants can freely operate windows. This model takes into account specific metabolic rates between 1.0 and 1.3 met and thermal resistance values of 0.5 clo in summer and 1.0 clo in winter.

The adaptive comfort temperature (T_{co}) is derived from the running mean dry bulb outdoor temperature ($T_{ext,ref}$), as defined in Equations (4) and (5). Based on this method three acceptability ranges can be defined depending on the building category: category I (PPD < 6 %) considers a temperature interval of + 2 °C - –3 °C; category II (PPD < 10%) establishes a temperature interval of + 3 °C - –4 °C; and, finally, category III (PPD < 15%) sets a temperature interval of + 4 °C - –5 °C. In this paper, building category II has been considered with a PPD lower than 10%.

$$T_{co} = 0.33 \times T_{ext,ref} + 18.8 \tag{4}$$

$$T_{ext,ref} = \left(T_{ext,ref\ 1} + 0.8\ T_{ext,ref\ 2} + 0.6\ T_{ext,ref\ 3} + 0.5\ T_{ext,ref\ 4} + 0.4\ T_{ext,ref\ 5} + 0.3\ T_{ext,ref\ 6} + 0.2\ T_{ext,ref\ 7}\right)/3.8 \tag{5}$$

where:
$T_{ext,ref}$: running mean dry bulb outdoor temperature for today
$T_{ext,ref1}$ to $T_{ext,ref7}$: daily mean dry bulb outdoor temperature for previous 1 to 7 days

For the application of this adaptive model, average outdoor running temperatures must be between 10 °C (lower limit) and 30 °C (upper limit). In this stage, annual indoor air temperatures in the social housing stock are predicted in an hourly-resolution through the energy simulation tool, considering the archetypes developed through the BSM (8,760 data points per number of simulations). Then, both hourly indoor and outdoor air predictions during a whole typical year are adequately imported to the Equations (4) and (5) of the adaptive thermal comfort model. Finally, the percentage of discomfort hours is obtained, determining the percentage of hours in the year that do not meet comfort conditions.

2.8. BSM sensitivity analysis.

In this last stage, a sensitivity analysis of the BSM has been conducted to determine the variables of the parameterized archectypes with the greatest influence on indoor thermal comfort at building stock level. In this second sensitivity analysis, the parameterized variables assessed are P1 to P25 (in Table 3 of section 2.6), since they define the building characterisation of the stock. Among

Table 3
Characterisation of case study and social housing H-building stock.

Variable	Description		BEM (case study)	BSM (AVRA database)	Distribution
General	–	Construction year	1973	1970–2005	–
	–	Building typology	H	H	–
	–	Spanish climatic zone	B4	B4	–
	–	Number of dwellings	26	5,935	–
Geometry	P1	Orientation (°)	53	0, ±30, ±60, 90	Uniform
	P2	Floor area (m^2)	78	60–122.50	Uniform
	P3	Floor height (m)	2.70	2.50–3.00	Uniform
	P4	Window-to-wall ratio (%)	14.5	10–30	Uniform
	P5	Number of stories	4	4–5	Uniform
Envelope	P6	Roof solar absorptance	0.55	0.1–0.9	Normal
	–	Roof U-value (W/m^2K)	2.29	1.2–2.4	–
	P7	Roof thickness (m)	0.30	0.25–0.40	Normal
	P8	Roof thermal conductivity (W/mK)	0.56	0.3–0.6	Normal
	P9	Roof density (kg/m^3)	1220	1000–1800	Normal
	P10	Roof specific heat (J/kgK)	1000	500–1500	Normal
	–	Floor U-value (W/m^2K)	3.60	3.0–7.00	–
	P11	Floor thickness (m)	0.25	0.15–0.30	Normal
	P12	Floor thermal conductivity (W/mK)	0.73	0.7–1.8	Normal
	P13	Floor density (kg/m^3)	1220	1200–1800	Normal
	P14	Floor specific heat (J/kgK)	1000	500–1500	Normal
	P15	Facade solar absorptance	0.70	0.1–0.9	Normal
	–	Facade U-value (W/m^2K)	1.52	1.2–2.5	–
	P16	Facade thickness (m)	0.25	0.10–0.35	Normal
	P17	Facade conductivity (W/mK)	0.20	0.2–0.4	Normal
	P18	Facade density (kg/m^3)	2170	1000–3000	Normal
	P19	Facade specific heat (J/kgK)	1000	500–1500	Normal
	P20	Partition thickness (m)	0.08	0.07–0.12	Normal
	P21	Type of window glass	Single	Single	Uniform
	P22	Type of window frame	Aluminium	Aluminium, Steel	Uniform
	–	Window U-value (W/m^2K)	5.70	5.50–5.70	–
Operation	P23	People density (people/m^2)	0.05	0.01–0.15	Normal
	P24	Infiltration rate (ACH)	0.53	0.30–1.00	Normal
	P25	Night-time natural ventilation rate (ACH)	0.3	0–4	Uniform

them, several variables which were not parameterized at the building level have been included (such as orientation, floor area, floor height, window-to-wall ratio and number of storeys) as they were considered fixed values during the calibration and validation processes of the BEM (first sensitivity analysis in subsection 2.4). Variables P1 to P25 have been considered in the ranges shown in Table 3 (current state of the stock). The methodology followed has already been explained in section 2.4.

The ultimate objective of including a sensitivity analysis at the social stock level is to be able to propose retrofit strategies in a future work line, focusing on the variables that report the most influential changes on thermal comfort assessment.

3. Results and discussion

3.1. BEM sensitivity analysis

Fig. 3 shows the classification of the studied variables based on the sensitivity analysis of the case study BEM, ranked according to the modified mean (μ^*) and standard deviation (σ). A total of 22 variables of the simulation model have been analysed and are described in the graph caption (1 to 22) . These variables include envelope parameters and physical properties of the building (thickness, thermal conductivity, density and specific heat of roof, façade and floor; solar absorptance of roof and façade; type of window glass and frame), as well as operational aspects (people density, infiltration rate, night-time natural ventilation rate). It should be pointed out that certain variables (orientation, floor area, floor height, window-to-wall ratio, number of stories) have not been parameterized in this model, given that their value is known with great precision and they have been considered as fixed values in the case study BEM for its calibration and validation. Likewise, the case study has no HVAC systems, so they have not been included in the BEM and, thus, no aspects relating HVAC systems have been assessed in this sensitivity analysis, evaluating the building's performance under free-running conditions.

Fig. 3 shows the variables with the greatest influence on the simulated indoor air temperatures in the top right-hand corner of the graph, representing the highest values of the standard deviation (σ) and modified mean (μ^*).

The top-4 (in decreasing order of influence) is composed of INFIL (infiltrations [ACH]), NV (natural ventilation [ACH]), PEOPLE (people density [people/m^2]) and FAÇADEt (façade thickness [m]). These four variables have been calibrated in the subsequent task. The opposite site of the graph ranks the following variables in ascending order of influence: FRAME (solar and visible absorptance of the window frame), FACADEd (density of the façade [kg/m^3]), GLAZc (conductivity of the glazing surface [W/m·K]) and ROOFc (conductivity of the roof [W/m·K]).

3.2. BEM Bayesian calibration

Fig. 4 shows the plausible posterior distributions (red histograms) of the calibration parameters of the BEM, which corresponds to the top-4 most influential variables in the simulation model described in subsection 3.1. Prior uncertainty distributions fixed as inputs during the calibration process are represented by the green lines (normal distributions). Blue lines indicate the most likely values reported in the Bayesian calibration (also normal distributions) when measurements observed (monitored data) were taken into account during the calibration process. If comparing prior and posterior distributions, it can be seen that all four parameters had to be finetuned in the model to make the proper adjustments, especially in the cases of NV (natural ventilation [ACH]) and

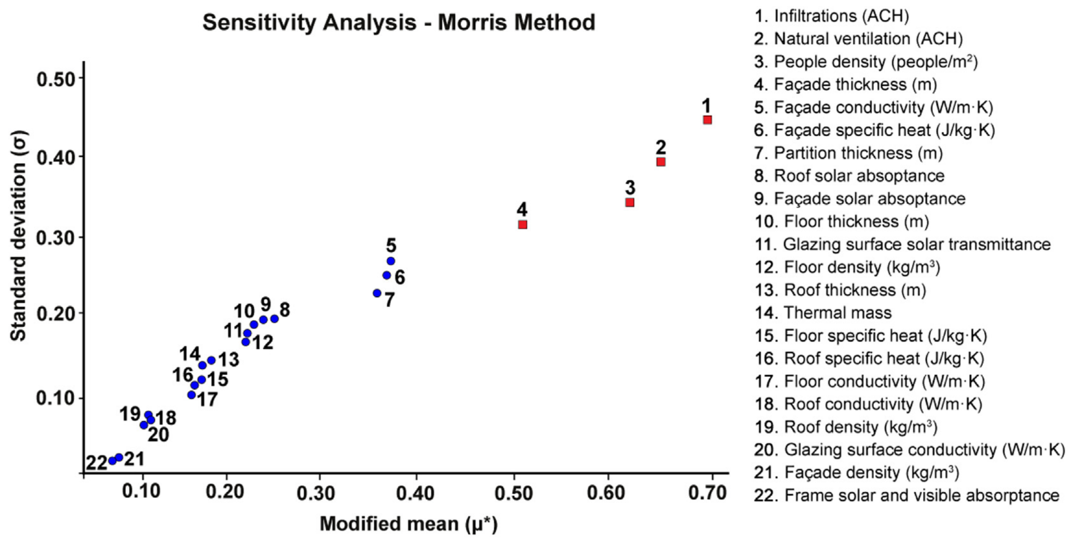

Fig. 3. Sensitivity analysis (Morris method) conducted on the BEM: identification of the most influential parameters on indoor air temperatures of the case study.

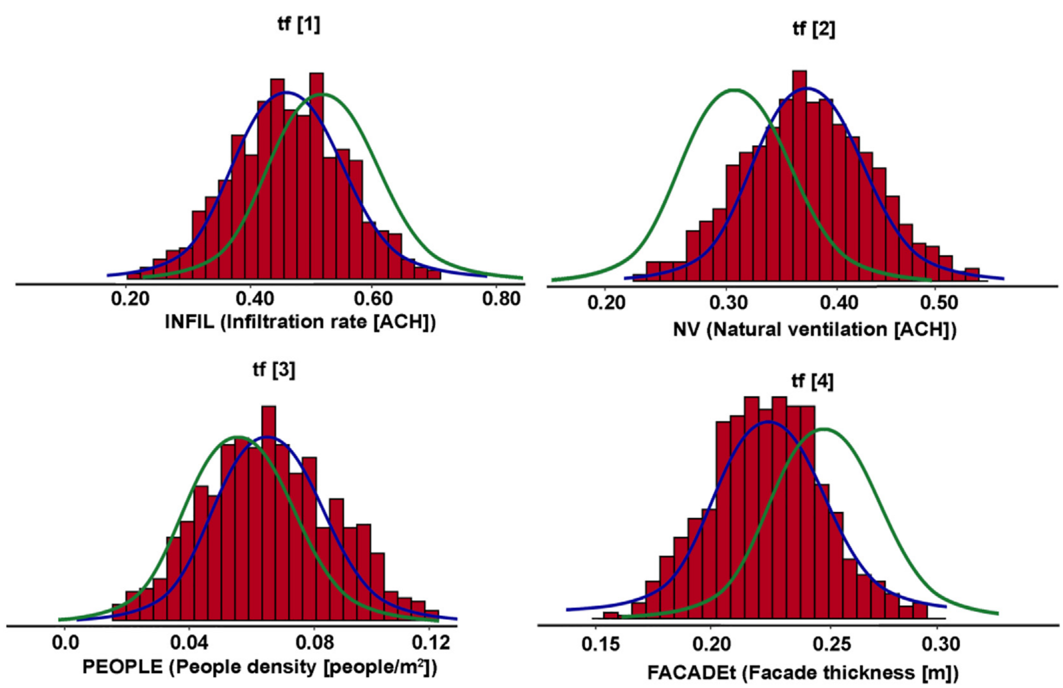

Fig. 4. Bayesian calibration of the BEM of the case study: posterior distributions (red histograms) determined from normal distributions (blue lines), for the top-4 most influential parameters (calibration parameters); green lines indicate prior distributions considered in the simulation model. (For interpretation of the references to colour in this figure legend, the reader is referred to the web version of this article.)

FACADEt (facade thickness [m]) parameters, which reported the most significant differences.

3.3. BEM validation

This section assesses the accuracy of the calibrated BEM of the case study. Thus, predicted hourly indoor air temperatures reported by the simulation model of the case study have been compared with on-site measurements. To do so, the 10-month monitored data have been classified in summer (June to September) and winter season (October to March), obtaining the statistical performance indices according to the ASHRAE Guideline 14:2002 [62]. No monitored data is available on April to May, so these months have not been included. Given the high-resolution of the data to be compared (hourly data), only a typical summer (4 to 10 of June) and winter (22 to 28 of December) weeks have been graphically represented in this paper.

The comparison between simulated and monitored data for the summer period is represented in Fig. 5a, while results from the winter period can be seen in Fig. 5b: blue lines represent on-site measurements; green lines refer to the simulation results of the uncalibrated model (previous to Bayesian calibration); and red lines indicate the simulated temperatures of the calibrated model (after Bayesian calibration). The uncertainty range (95% confidence) of the posterior distributions has been also included in the figure (grey).

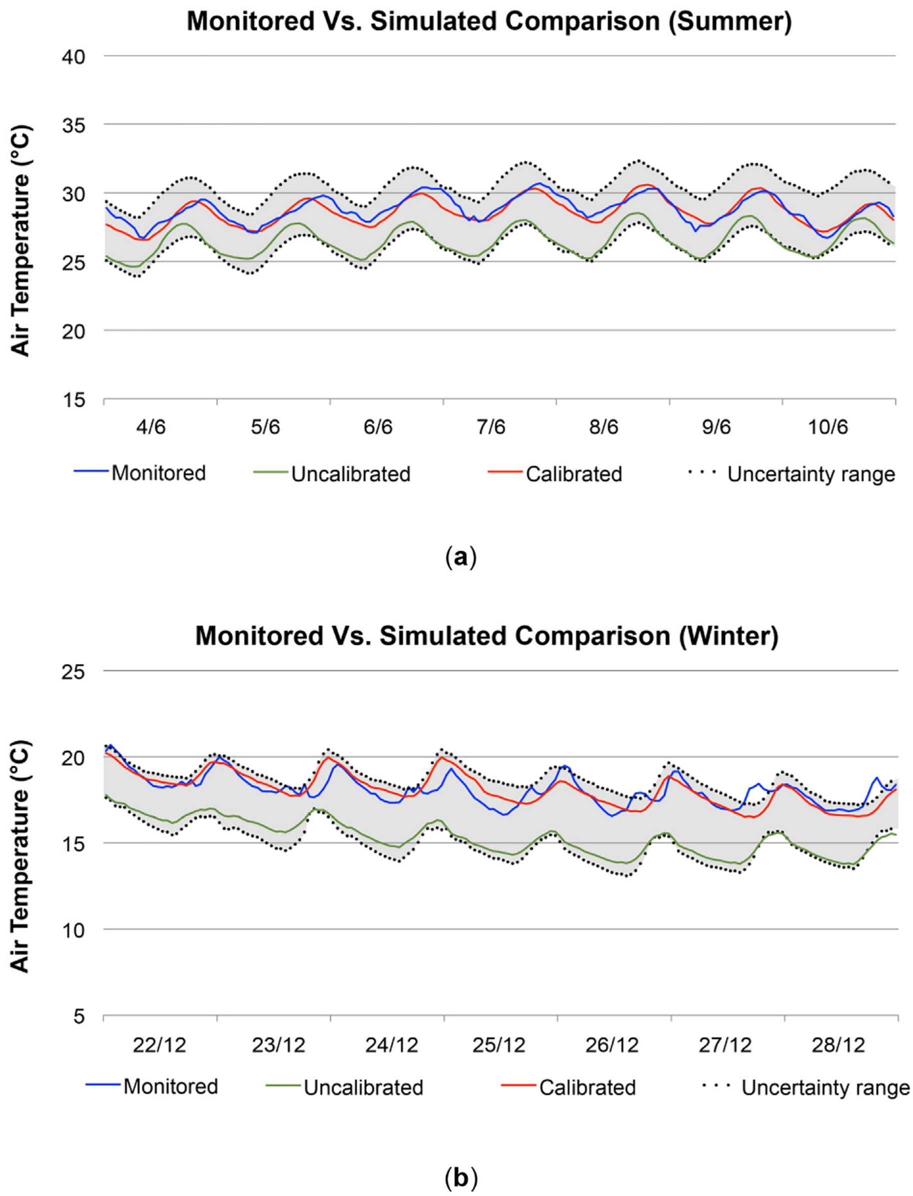

Fig. 5. Comparison of on-site measurements and simulation results of the BEM of the case study during: (**a**) summer; (**b**) winter. The green and red lines represent the prediction of the un-calibrated and calibrated models, respectively. Blue lines refer to monitored data. The uncertainty range (95% confidence intervals) relating to the posterior distributions of the calibrated model is shown in grey. (For interpretation of the references to colour in this figure legend, the reader is referred to the web version of this article.)

Fig. 5 shows a clear improvement in the quality of the simulation model after the calibration process, obtaining hourly-simulated results closer to the monitored data. On-site measurements are within the 95% confidence uncertainty ranges of the calibrated model (grey) in both summer and winter, determined from the variations within posterior distribution ranges. ASHRAE statistical indices have been calculated for both periods (Table 4).

When comparing these indices prior to and after calibration, it can be observed that all of them are below the thresholds established in the international standard, significantly improving the model (by around 81–90% in summer and 73–85% in winter). Bearing in mind these results, the case study BEM is considered to be adequately calibrated and validated.

Table 5 shows the calculation of annual adaptive thermal comfort, for the case study (taking into consideration on-site hourly air temperature measurements) and the calibrated BEM model (obtained from the hourly air temperature simulated outputs). Adaptive thermal comfort has been determined according to the procedure included in the EN 16798–1:2019 [38].

Table 4
Uncertainty indices obtained for summer and winter periods (hourly calibration frequency).

Period	Model	NMBE (±10%)	CVRMSE (<30%)	R^2 (>0.75)
Summer	Un-calibrated	7.90	8.50	0.36
	Calibrated	0.66	1.61	0.82
Winter	Un-calibrated	13.00	14.10	0.58
	Calibrated	1.87	3.74	0.75

Table 5
Comparison of thermal comfort calculated from on-site measurements and simulated outputs.

Model	Discomfort hours in winter (%)	Discomfort hours in summer (%)	Annual discomfort hours (%)
Case study	81.7	23.5	57.3
Calibrated BEM	80.1	31.7	64.0

It can be seen that the calibrated model predicts a percentage of discomfort hours in winter quite close to the one obtained in the case study. Nevertheless, during the summer season, the calibrated BEM model over predicts discomfort hours, reporting values not within the adaptive comfort band during 8.2% more hours. This leads to a difference in the percentage of annual discomfort hours reported in the case study (57.3% discomfort hours) and the calibrated BEM (64.0% discomfort hours) of 6.7%, with the BEM overpredicting indoor temperatures. The highest temperature difference registered between the case study and the calibrated BEM is 1.96 °C during the summer season.

3.4. Thermal comfort assessment of the current social housing building stock

Fig. 6 shows the percentage of annual discomfort hours (%) on the Y-axis, obtained from the analysis of the current thermal performance of the H-typology social housing stock in southern Spain, assessed through the parameterized BSM archetypes (described in subsection 2.6).

Comparison results are represented for different numbers of simulated cases (X-axis: 250, 500, 750 and 1000 simulations). To do so, box-and-whisker plots have been used to represent the dispersion of the samples: the lower and upper whiskers indicate the minimum and maximum values of the sample, respectively; the horizontal edges of the rectangle are the interquartile range (third quartile – first quartile), so that 25% of the data are represented up to the lower horizontal edge (first quartile), while 75% of the sample is included up to the upper horizontal edge (third quartile); the horizontal line inside the rectangle represents the second quartile (50% of the data, also the median). The black dashed line joins the average percentage of the annual discomfort hours of each analysed sample (represented with a black cross and indicated in red at the top of each box).

In terms of thermal comfort, it can be observed that annual discomfort hours for the building stock analysed (H-typology in southern Spain, in its current state) are generally between 54.5% and 76.5% (with punctual outlier values in each sample set). However, values are occasionally recorded outside the interquartile range, reaching 52.0% annual discomfort hours. The annual average values of discomfort hours which are generated for each simulation sample are quite close together (68.3 % and 68.4%), and similar to the percentage obtained for the case study (71.5%), which is within the maximum values.

Another aspect to be highlighted is that the values of annual discomfort hours obtained in the four simulation cases (250, 500, 750 and 1000 simulations) are significantly close and follow a similar trend. Thus, results obtained with the parameterized models are quite representative with a reduced number of simulations (250 against 1000 simulations). Considering these results, analysing a minimum number of 10 LHS per parameterized variables (in this case, 250 simulations) would report significant results for the building stock analysed. This has the advantage of noticeably reducing computational costs: the analysis of 250 annual simulations of whole buildings required a 3-hour computational period, whereas when the simulation number was increased to 1000 building models, computational time was around 14 h (considering a computer with i7-8700 CPU 3.20 GHz of 12 cores and 16 GB RAM).

Fig. 7 shows the average percentages of comfort and discomfort hours obtained for both summer (May to September, 3,672 h analysed) and winter (October to April 5088 h analysed), as well as the average annual values (8,760 h analysed). Discomfort results have been classified in undercooling hours (indoor temperatures below the lower comfort limit) and overheating hours (indoor temperatures above the upper comfort limit).

In average, 45.4% of 3,672 summer hours are in discomfort conditions, while 91.7% of the 5,088 winter hours are in discomfort, which lead to an average annual discomfort value of 68.3%. The percentage of annual undercooling hours is significantly higher than that of overheating hours, 57.7% in contrast to 10.6%. Overheating in winter only occurs 0.1% of the discomfort hours, while undercooling takes place 18.2% of the discomfort hours in summer. When analysing the case study, it suffers from annual undercooling during 68.3% of the total discomfort hours, with only 3% of overheating discomfort hours.

3.5. BSM sensitivity analysis

Fig. 8 represents the results from the sensitivity analysis carried out to determine the most influential variables of the BSM of the H-typology social housing stock in southern Spain on indoor annual thermal comfort, considering the ranges obtained from its building characterisation in its current state (variables P1 to P25, with the

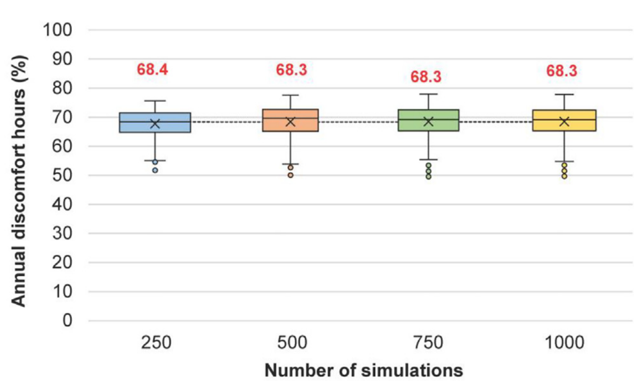

Fig. 6. Thermal comfort assessment of H-typology social housing stock in southern Spain: comparison of the percentage of annual discomfort hours when different simulation runs are considered.

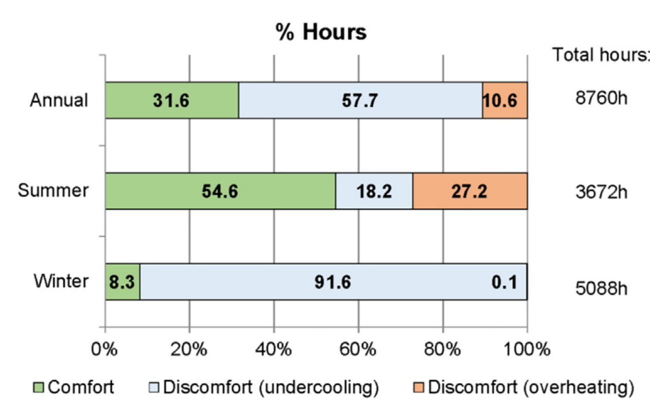

Fig. 7. Average percentages of comfort and discomfort (undercooling and overheating) hours obtained per each seasonal period and per year. Results were obtained from 250 simulations.

sampling distribution shown in Table 3 of section 2.6). As with the BEM in section 3.1, the parameterized variables P1 to P25 of the BSM have been ranked according to the modified mean (μ^*) and standard deviation (σ), so that the most influential parameters are located on the top-right corner (highest $\mu^*$and σ) of the figure. The top-ten most influential variables are shown in red, while those with the lowest repercussion on indoor thermal comfort are represented in blue.

This figure shows the top-3 of the variables with the highest influence on indoor thermal comfort of the BSM: P24. Infiltration rate (ACH), P23. People density (people/m^2) and P25. Night-time natural ventilation rate (ACH). Other variables also with great interest on comfort are, in decreasing importance order: P1. Orientation (°), P4. Window-to-wall ratio (%), P16.Facade thickness (m), P11. Floor thickness (m), P6. Roof solar absorptance, P17. Façade conductivity (W/m·K) and P12. Floor thermal conductivity (W/m·K). Among the 25 variables analysed, those with the lowest significance on indoor thermal comfort are P15. Façade solar absorptance and P9. Roof density (kg/m^3).

Several studies have reported conclusions regarding the most influential variables in BEM. However, this is normally done at single building level for energy aspects: Yang et al. [54] analyse 13 parameters related to envelope properties, internal loads and HVAC systems for a single building case study located in Shanghai, reporting that the chiller COP, lighting/equipment power density and occupant density are the most influential variables on average energy consumption; the study by Chong et al. [60] of an office building in Singapore identifies the parameters with the greatest influence as lighting and equipment power density, fan pressure and efficiency and cooling set point, from a total of 28 parameters of envelope properties, internal loads and HVAC system characteristics. Abokersh et al. [61] consider 31 parameters (input climate data, building envelope, HVAC system and operational aspects) for a two-storey dwelling in the Netherlands and report that the variables with the highest impact on energy thermal consumption and hours when operating temperatures are not within the thermal comfort static band of 20–24 ° are infiltration, thermal mass fraction, window opening angle and windows G-value. Yuan et al. [72] assess 10 parameters relating to the envelope, internal loads, ventilation and cooling systems of an office building in Singapore, concluding that the COP of the cooling plant, window and wall U-values, ventilation rate and equipment / lighting power density are the most influential variables on the building energy performance. When considering free-running conditions and thermal comfort assessment, Escandón et al. [71] report similar results to those obtained in this research, but for linear-type social housing in southern Spain. After analysing 29 variables (geometry, operation and envelope parameters), the authors report natural ventilation, people density, infiltration, orientation and building area as the top-5 most influential parameters on annual thermal comfort.

4. Strengths and limitations. Future research

It should be borne in mind that this research only presents results for indoor thermal comfort of the H-typology social housing stock in southern Spain in its current state, using statistical data from the building characterisation from a public housing database. Nevertheless, the assessment of this building stock through parameterized energy simulation models allows this analysis to be spread to other interesting variables, such as energy demand or consumption.

This paper also shows specific results for the B4 Spanish climate zone, as described in the methodology section, which directly influences the determination of the variation ranges of the parameters relating to building stock characterisation. Nonetheless, the application of the same methodological approaches to the analysis could be extended to other different climate zones in southern Spain, generating energy models representative of other climate areas, based on their building characterisation (data also contained in the public social housing database used).

Similarly, building environments could also be parameterized by applying the hybrid bottom-up approach proposed in this study at urban level, with lower computational costs than district level analysis, in order to assess the influence of environment elements on the indoor spaces of the buildings (i.e. shading effects of close buildings).

Another drawback is the limited weather data that were included into the weather file (.epw) linked to the energy model simulation file for the calibration process. Only information

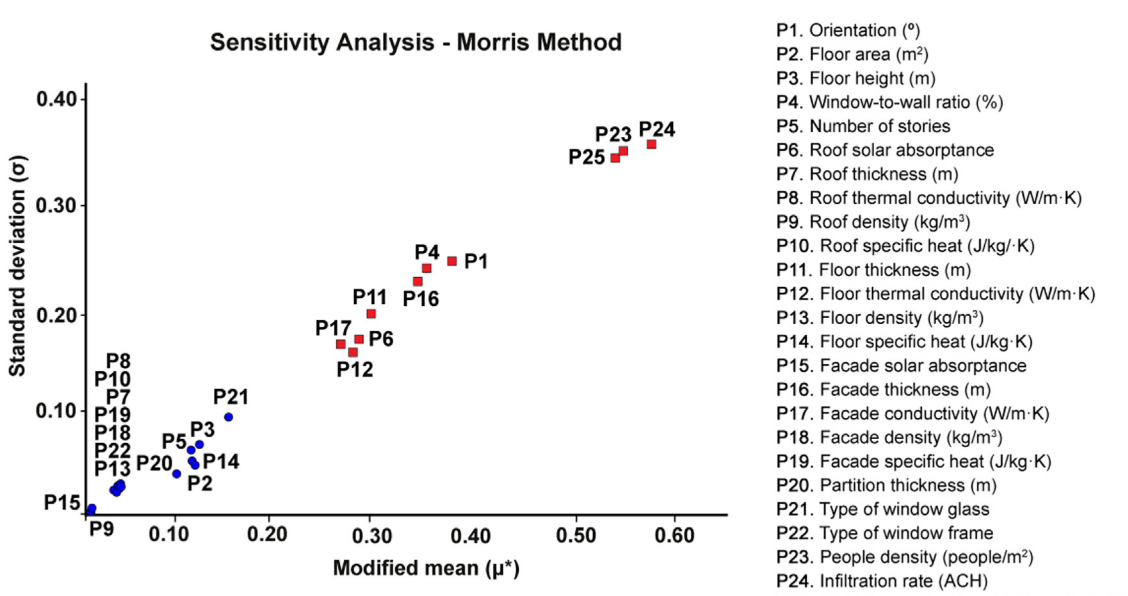

Fig. 8. Sensitivity analysis (Morris method) conducted on the BSM: determination of the most influential parameters on annual thermal comfort of H-typology social housing stock.

regarding hourly outdoor temperatures was available. Thus, essential information related to solar radiation levels, outdoor illuminance or sky cover were missing. Even though calibration results obtained were within the validation regulation thresholds, future works should assess the incorporation of more information on local weather data through on-site monitoring for the calibration process.

The use of parameterized energy models to assess thermal and energy performance in the building sector in view of future climate change scenarios and the proposal of optimized energy retrofit measures at stock level are also other possible scopes of research. These may report useful results for decision-making in the public administration and will be the focus of future publications. Thus, combining parameterized energy models with screening techniques, as has been done in this paper, is of great importance, as this approach can focus calibration efforts of energy models or future retrofit strategies on the parameters reporting the highest impact on the simulated outputs.

Even though, calibration and validation processes were conducted comparing indoor air temperatures, monitored during a high-resolution and long-term period, with predicted indoor temperatures, no calibration and validation on thermal comfort predictions were conducted, as no comfort data were available during the monitoring stage. Future works ought to consider the possibility of calibrating and validating BSM based on thermal comfort surveys and information.

5. Conclusions

This paper assesses the current performance in terms of indoor thermal comfort of the social housing building stock in southern Spain (Mediterranean climate), considering one of the most representative building typologies of this sector, the H-typology. This is done by combining on-site monitoring methods with energy modelling and statistical techniques for data analysis. The hybrid bottom-up approach implemented considers the building characterisation of the housing stock analysed, from which a case study is selected, monitored and modelled. This case study is then calibrated following the Bayesian technique and validated according to international standards to generate parameterized energy models representative of the social housing buildings, allowing energy simulation and assessment at stock level. This is achieved through a physical, constructive, morphological and geometrical characterisation of the building stock, using statistical methods for analysis and incorporating the results obtained into the parameterized building energy models.

One of the main conclusions reached in this research is the average percentage of annual discomfort hours of the stock analysed in its current state, approximately 68%, of which close to 58% are caused by undercooling hours. This is due to the fact that winter period is 16% longer than the summer season, so the percentage of discomfort hours is higher.

Moreover, the variables of the stock models with the greatest impact on these results, obtained through sensitivity analysis, are (in order of decreasing importance): the infiltration rate (ACH), people density (people/m^2) and night-time natural ventilation rate (ACH). In contrast, the variables of the model at the BSM level with the lowest influence on indoor thermal comfort are façade solar absorptance and roof density (kg/m^3), among a total of 25 parameters.

It must also be stressed that this study has also allowed the significance of the predicted results obtained to be tested using a minimum number of simulations equal to 10 LHS per parameterized variable, in order to adequately assess the social housing stock. For a sample of 250 simulation cases (3-hour computational time) the percentage of annual discomfort hours obtained is 68.4%, close to those reported after 14 h of calculation for 1000 simulation cases, 68.3%, and for the single building case study (71.5%). This fact has the advantage of significantly reducing computational burdens, while maintaining the representativeness of the predicted results.

Author Contributions

All authors have conceived and designed the experiments, performed the experiments, analysed the data and written, reviewed and approved the final manuscript.

Declaration of Competing Interest

The authors declare that they have no known competing financial interests or personal relationships that could have appeared to influence the work reported in this paper.

Acknowledgements

The authors wish to acknowledge the financial support provided by the Spanish Ministry of Economy and Competitiveness and the European Regional Development Fund through the research project "Parametric Optimisation of Double Skin Facades in the Mediterranean Climate for the Improvement of Energy Efficiency in Climate Change Scenarios" (BIA2017-86383-R). Calama-González also acknowledges the support of the FPU Program of the Spanish Ministry of Education, Culture and Sport (FPU17/01375).

References:

[1] NASA U.S. National Aeronatics and Space Administration Earth Science Communications Team. Global Climate Change: Vital Signs of the Planet https://climate.nasa.gov/vital-signs/global-temperature/ [accessed March 2021].
[2] European standards committee. EN 16798-7:2019 Energy Performance of Buildings – Ventilation for buildings - Part 7: Calculation methods for determination of air flow rates in buildings including infiltration - Module M5–5. 2019.
[3] EU Commission and Parliament, Directive 2010/31/EU of the European Parliament and of the Council of 19 May 2010 on the energy performance of buildings https://eur-lex.europa.eu/legal-content/EN/TXT/?uri=celex%3A32010L0031 [accessed March 2021].
[4] Hartless R. Application of energy performance regulations to existing buildings. Final report of the Task B4, ENPER TEBUC Project 2003.
[5] EU Commission and Parliament, Communication from the Commission to the European parliament, The European Council, the Council, The European Economic and Social Committee and the Committee of the Regions. The European Green Dela COM/2019/640 final https://eur-lex.europa.eu/legal-content/EN/TXT/?qid=1588580774040&uri=CELEX:52019DC0640 [accessed March 2021].
[6] É. Mata, A. Sasic Kalagasidis, F. Johnsson, Building-stock aggregation through archetype buildings: France, Germany, Spain and the UK. Build Environ (2014), https://doi.org/10.1016/j.buildenv.2014.06.013.
[7] International Energy Agency. Tracking buildings 2020 https://www.iea.org/reports/tracking-buildings-2020 [accessed March 2021].
[8] G.G. Akkurt, N. Aste, J. Borderon, A. Buda, M. Calzolari, D. Chung, et al., Dynamic thermal and hygrometric simulation of historical buildings: Critical factors and possible solutions, Renew Sustain Energy Rev (2020), https://doi.org/10.1016/j.rser.2019.109509.
[9] E. Azar, W. O'Brien, S. Carlucci, T. Hong, A. Sonta, J. Kim, et al., Simulation-aided occupant-centric building design: A critical review of tools, methods, and applications, Energy Build (2020), https://doi.org/10.1016/j.enbuild.2020.110292.
[10] M. Sunikka-Blank, R. Galvin, Introducing the prebound effect: The gap between performance and actual energy consumption, Build Res Inf (2012), https://doi.org/10.1080/09613218.2012.690952.
[11] T. Hong, J. Langevin, K. Sun, Building simulation: Ten challenges. Build Simul (2018), https://doi.org/10.1007/s12273-018-0444-x.
[12] J. Schiefelbein, J. Rudnick, A. Scholl, P. Remmen, M. Fuchs, D. Müller, Automated urban energy system modeling and thermal building simulation based on OpenStreetMap data sets, Build Environ (2019), https://doi.org/10.1016/j.buildenv.2018.12.025.

[13] L.G. Swan, V.I. Ugursal, Modeling of end-use energy consumption in the residential sector: A review of modeling techniques, Renew Sustain Energy Rev (2009), https://doi.org/10.1016/j.rser.2008.09.033.
[14] F. Ascione, N. Bianco, G.M. Mauro, D.F. Napolitano, Knowledge and energy retrofitting of neighborhoods and districts. A comprehensive approach coupling geographical information systems, building simulations and optimization engines, Energy Convers Manag (2021), https://doi.org/10.1016/j.enconman.2020.113786.
[15] C.F. Reinhart, D.C. Cerezo, Urban building energy modeling - A review of a nascent field, Build Environ (2016), https://doi.org/10.1016/j.buildenv.2015.12.001.
[16] A. Mastrucci, O. Baume, F. Stazi, U. Leopold, Estimating energy savings for the residential building stock of an entire city: A GIS-based statistical downscaling approach applied to Rotterdam, Energy Build (2014), https://doi.org/10.1016/j.enbuild.2014.02.032.
[17] K. Amasyali, N.M. El-Gohary, A review of data-driven building energy consumption prediction studies, Renew Sustain Energy Rev (2018), https://doi.org/10.1016/j.rser.2017.04.095.
[18] Moffat, S. Stock Aggregation: Methods for Evaluation the Environmental Performance of Building Stocks. Report for IEA Annex 31: Energy-related environmental impact of buildings, 2004.
[19] Use of building typologies for energy performance assessment of national building stocks. existent experiences in European countries a common approach - First Tabula synthesis report: 'Use of building typologies for energy performance assessment of national building stocks. Existent experiences in European countries and common approach https://www.episcope.eu/downloads/public/docs/report/TABULA_SR1.pdf [accessed March 2021].
[20] C. Ahern, B. Norton, A generalisable bottom-up methodology for deriving a residential stock model from large empirical databases, Energy Build (2020), https://doi.org/10.1016/j.enbuild.2020.109886.
[21] S. Farzana, M. Liu, A. Baldwin, M.U. Hossain, Multi-model prediction and simulation of residential building energy in urban areas of Chongqing, South West China. Energy Build (2014), https://doi.org/10.1016/j.enbuild.2014.06.007.
[22] J. Mikkola, P.D. Lund, Models for generating place and time dependent urban energy demand profiles, Appl Energy (2014), https://doi.org/10.1016/j.apenergy.2014.05.039.
[23] M. Krarti, M. Aldubyan, E. Williams, Residential building stock model for evaluating energy retrofit programs in Saudi Arabia, Energy (2020), https://doi.org/10.1016/j.energy.2020.116980.
[24] M. Österbring, É. Mata, L. Thuvander, M. Mangold, F. Johnsson, H. Wallbaum, A differentiated description of building-stocks for a georeferenced urban bottom-up building-stock model, Energy Build (2016), https://doi.org/10.1016/j.enbuild.2016.03.060.
[25] F. Ascione, R.F. De Masi, F. de Rossi, R. Fistola, M. Sasso, G.P. Vanoli, Analysis and diagnosis of the energy performance of buildings and districts: Methodology, validation and development of Urban Energy Maps, Cities (2013), https://doi.org/10.1016/j.cities.2013.04.012.
[26] M. Issermann, F.J. Chang, P.Y. Kow, Interactive urban building energy modelling with functional mockup interface of a local residential building stock, J Clean Prod (2021), https://doi.org/10.1016/j.jclepro.2020.125683.
[27] T. Loga, B. Stein, N. Diefenbach, TABULA building typologies in 20 European countries—Making energy-related features of residential building stocks comparable, Energy Build (2016), https://doi.org/10.1016/j.enbuild.2016.06.094.
[28] C. Nägeli, M. Jakob, G. Catenazzi, Y. Ostermeyer, Towards agent-based building stock modeling: Bottom-up modeling of long-term stock dynamics affecting the energy and climate impact of building stocks, Energy Build (2020), https://doi.org/10.1016/j.enbuild.2020.109763.
[29] U. Filippi Oberegger, R. Pernetti, R. Lollini, Bottom-up building stock retrofit based on levelized cost of saved energy, Energy Build (2020), https://doi.org/10.1016/j.enbuild.2020.109757.
[30] M. Brøgger, P. Bacher, K.B. Wittchen, A hybrid modelling method for improving estimates of the average energy-saving potential of a building stock, Energy Build (2019), https://doi.org/10.1016/j.enbuild.2019.06.054.
[31] J.A. Fonseca, T.A. Nguyen, A. Schlueter, F. Marechal, City Energy Analyst (CEA): Integrated framework for analysis and optimization of building energy systems in neighborhoods and city districts, Energy Build (2016), https://doi.org/10.1016/j.enbuild.2015.11.055.
[32] R. Escandón, R. Suárez, J.J. Sendra, Field assessment of thermal comfort conditions and energy performance of social housing: The case of hot summers in the Mediterranean climate, Energy Policy (2019), https://doi.org/10.1016/j.enpol.2019.01.009.
[33] T. Blázquez, S. Ferrari, R. Suárez, J.J. Sendra, Adaptive approach-based assessment of a heritage residential complex in southern Spain for improving comfort and energy efficiency through passive strategies: A study based on a monitored flat, Energy (2019), https://doi.org/10.1016/j.energy.2019.05.160.
[34] I.G. Dino, A.C. Meral, Impact of climate change on the existing residential building stock in Turkey: An analysis on energy use, greenhouse gas emissions and occupant comfort, Renew Energy (2019), https://doi.org/10.1016/j.renene.2019.03.150.
[35] Ansi/Ashrae. ANSI/ASHRAE 55:2004 Thermal Environmental Conditions for Human Occupancy. ASHRAE 2004.
[36] BS EN 15251. Indoor environmental input parameters for design and assessment of energy performance of buildings-addressing indoor air quality, thermal environment, lighting and acoustics 2007.
[37] P. Palma, J.P. Gouveia, S.G. Simoes, Mapping the energy performance gap of dwelling stock at high-resolution scale: Implications for thermal comfort in Portuguese households, Energy Build (2019), https://doi.org/10.1016/j.enbuild.2019.03.002.
[38] European standards committee. EN 16798-1:2019 Energy Performance of Buildings – Ventilation for buildings - Part 1: Indoor Environmental Input Parameters for Design and Assessment of Energy Performance of Buildings Addressing Indoor Air Quality, Thermal Environment, Lighting and Acoustics - Module M1–6. 2019.
[39] AVRA Andalusian Agency of House and Retrofitting (Agencia de Vivienda y Rehabilitación de Andalucía, in Spanish) http://www.juntadeandalucia.es/avra [accessed March 2021].
[40] Online Cadastrial Office (Sede Electrónica del Catastro, in Spanish) https://www.sedecatastro.gob.es [accessed March 2021].
[41] Spanish Technical Building Code Basic Document: Energy Savings (Código Técnico de la Edificación. Documento Básico: Ahorro de Energía, in Spanish) 2019 Spanish Government Madrid Spain https://www.codigotecnico.org [accessed March 2021].
[42] C.M. Calama-González, R. Suárez, A.L. León-Rodríguez, Building characterisation and assessment methodology of social housing stock in the warmer Mediterranean climate: The case of southern Spain, IOP Conf. Ser. Earth Environ. Sci. (2020), https://doi.org/10.1088/1755-1315/410/1/012049.
[43] Microsoft Excel 2016® Microsoft Redmond WA USA
[44] R v.3.5.3. R Core Team. GNU GPL v2 https://www.r-project.org/ [accessed March 2021].
[45] Quantum GIS Geographic Information System v.2.18. Development Team. Open Source Geospatial Foundation Project. 2015. Las Palmas de Gran Canaria Spain.
[46] Blázquez de Pineda, M. T. (2019). Energy characterization and comfort conditions in Rafael De La Hoz's social housing in Córdoba. Scenarios for improvement. PhD, University of Seville https://hdl.handle.net/11441/89977 [accessed March 2021].
[47] U.S. Department of Energy. EnergyPlus Energy Simulation Software, 2017 http://apps1.eere.energy.gov/buildings/energyplus [accessed March 2021].
[48] P. De Wilde, The gap between predicted and measured energy performance of buildings: A framework for investigation, Autom Constr (2014), https://doi.org/10.1016/j.autcon.2014.02.009.
[49] G.R. Ruiz, C.F. Bandera, Validation of calibrated energy models: Common errors, Energies (2017), https://doi.org/10.3390/en10101587.
[50] Zhang Y, Korolija I. jEPlus - An EnergyPlus simulation manager for parametrics. jEPlus 1.7.2. 2016. http://sourceforge.net/projects/[accessed March 2021].
[51] S. Martínez, A. Erkoreka, P. Eguía, E. Granada, L. Febrero, Energy characterization of a PASLINK test cell with a gravel covered roof using a novel methodology: Sensitivity analysis and Bayesian calibration, J Build Eng (2019), https://doi.org/10.1016/j.jobe.2018.11.010.
[52] M.D. Morris, Factorial sampling plans for preliminary computational experiments, Technometrics (1991), https://doi.org/10.1080/00401706.1991.10484804.
[53] F. Campolongo, J. Cariboni, A. Saltelli, An effective screening design for sensitivity analysis of large models, Environ Model Softw (2007), https://doi.org/10.1016/j.envsoft.2006.10.004.
[54] T. Yang, Y. Pan, J. Mao, Y. Wang, Z. Huang, An automated optimization method for calibrating building energy simulation models with measured data: Orientation and a case study, Appl Energy (2016), https://doi.org/10.1016/j.apenergy.2016.07.084.
[55] M.H. Kristensen, S. Petersen, Choosing the appropriate sensitivity analysis method for building energy model-based investigations, Energy Build (2016), https://doi.org/10.1016/j.enbuild.2016.08.038.
[56] C.M. Calama-González, P. Symonds, G. Petrou, R. Suárez, Á.L. León-Rodríguez, Bayesian calibration of building energy models for uncertainty analysis through test cells monitoring, Appl Energy (2021), https://doi.org/10.1016/j.apenergy.2020.116118.
[57] A. Chong, K. Menberg, Guidelines for the Bayesian calibration of building energy models, Energy Build (2018), https://doi.org/10.1016/j.enbuild.2018.06.028.
[58] M.C. Kennedy, A. O'Hagan, Bayesian calibration of computer models, J R Stat Soc Ser B Stat Methodol (2001), https://doi.org/10.1111/1467-9868.00294.
[59] J. Chen, X. Gao, Y. Hu, Z. Zeng, Y. Liu, A meta-model-based optimization approach for fast and reliable calibration of building energy models, Energy (2019), https://doi.org/10.1016/j.energy.2019.116046.
[60] A. Chong, W. Xu, S. Chao, N.T. Ngo, Continuous-time Bayesian calibration of energy models using BIM and energy data, Energy Build (2019), https://doi.org/10.1016/j.enbuild.2019.04.017.
[61] M.H. Abokersh, M. Spiekman, O. Vijlbrief, T.A.J. van Goch, M. Vallès, D. Boer, A real-time diagnostic tool for evaluating the thermal performance of nearly zero energy buildings, Appl Energy (2021), https://doi.org/10.1016/j.apenergy.2020.116091.
[62] ANSI/ASHRAE. ASHRAE Guideline 14-2002 Measurement of Energy and Demand Savings. ASHRAE 2002.
[63] J.C. Helton, J.D. Johnson, C.J. Sallaberry, C.B. Storlie, Survey of sampling-based methods for uncertainty and sensitivity analysis, Reliab Eng Syst Saf (2006), https://doi.org/10.1016/j.ress.2005.11.017.

[64] J.C. Helton, F.J. Davis, J.D. Johnson, A comparison of uncertainty and sensitivity analysis results obtained with random and Latin hypercube sampling, Reliab Eng Syst Saf (2005), https://doi.org/10.1016/j.ress.2004.09.006.
[65] Z. Pang, Z. O'Neill, Y. Li, F. Niu, The role of sensitivity analysis in the building performance analysis: A critical review, Energy Build (2020), https://doi.org/10.1016/j.enbuild.2019.109659.
[66] P. Westermann, M. Welzel, R. Evins, Using a deep temporal convolutional network as a building energy surrogate model that spans multiple climate zones, Appl Energy (2020), https://doi.org/10.1016/j.apenergy.2020.115563.
[67] H. Li, S. Wang, H. Cheung, Sensitivity analysis of design parameters and optimal design for zero/low energy buildings in subtropical regions, Appl Energy (2018), https://doi.org/10.1016/j.apenergy.2018.07.023.
[68] G. Tardioli, A. Narayan, R. Kerrigan, M. Oates, J. O'Donnell, D.P. Finn, A methodology for calibration of building energy models at district scale using clustering and surrogate techniques, Energy Build (2020), https://doi.org/10.1016/j.enbuild.2020.110309.
[69] J. Mao, J.H. Yang, A. Afshari, L.K. Norford, Global sensitivity analysis of an urban microclimate system under uncertainty: Design and case study, Build Environ (2017), https://doi.org/10.1016/j.buildenv.2017.08.011.
[70] J.L. Loeppky, J. Sacks, W.J. Welch, Choosing the sample size of a computer experiment: A practical guide, Technometrics (2009), https://doi.org/10.1198/TECH.2009.08040.
[71] R. Escandón, F. Ascione, N. Bianco, G.M. Mauro, R. Suárez, J.J. Sendra, Thermal comfort prediction in a building category: Artificial neural network generation from calibrated models for a social housing stock in southern Europe, Appl Therm Eng (2019), https://doi.org/10.1016/j.applthermaleng.2019.01.013.
[72] J. Yuan, V. Nian, B. Su, Q. Meng, A simultaneous calibration and parameter ranking method for building energy models, Appl Energy (2017), https://doi.org/10.1016/j.apenergy.2017.08.220.